

# Mobility Crossover in Two-Dimensional Berry Crystals

Zixuan Chai,<sup>1,2,\*</sup> Si-Yuan Chen,<sup>2,3,†</sup> Chenzheng Yu,<sup>3,4,‡</sup> Anton M. Graf,<sup>5,4</sup> Joonas Keski-Rahkonen,<sup>4,2</sup> and Eric J. Heller<sup>4,2,§</sup>

<sup>1</sup>*Department of Physics, University of Cambridge, Cambridge, UK*

<sup>2</sup>*Department of Physics, Harvard University, Cambridge, Massachusetts 02138, USA*

<sup>3</sup>*International Center for Quantum Materials and School of Physics, Peking University, Beijing 100871, China*

<sup>4</sup>*Department of Chemistry and Chemical Biology,*

*Harvard University, Cambridge, Massachusetts 02138, USA*

<sup>5</sup>*Harvard John A. Paulson School of Engineering and Applied Sciences, Harvard, Cambridge, Massachusetts 02138, USA*

(Dated: March 3, 2026)

A Berry crystal is a random superposition of  $N$  plane waves of equal amplitude and fixed wavevector magnitude, propagating in different directions. Using numerical simulations of wavepacket dynamics, spectral analysis based on autocorrelation functions, and scaling of Inverse Participation Ratio, the nature of eigenstates across the energy spectrum of a two-dimensional Berry crystal is characterized. It exhibits Anderson localization and critical (extended but non-ergodic) states, reminiscent of quasicrystals, which sit in the middle ground between periodic and disordered systems and can host critical states. However, in contrast to quasicrystals that display sharp mobility edges separating extended and localized phases, the Berry crystal exhibits an extended regimes of critical states. We name this a "mobility crossover". At weak potential strength, low-energy states are extended while higher-energy states near the backscattering momentum are critical. As the potential strength increases to become comparable with the recoil energy, these critical states evolve into localized states, yielding a transition from extended non-ergodic to localized behavior near the backscattering momentum. An estimate for the boundaries of ergodic extended regimes is given by the mapping onto an effective Anderson model on a Bethe Lattice. The results shed light on the relation between backscattering and Anderson localization in continuous two-dimensional aperiodic systems.

## INTRODUCTION

Anderson localization (AL) is a phenomenon that describes the ubiquitous existence of exponentially localized energy eigenstates in disordered systems [1]. AL presents in many kinds of systems.

In tight-binding models with uncorrelated disorders in onsite energies, scaling theory predicts that all states are localized in one and two dimensions, while a metal-insulator transition occurs in three dimensions (1D and 2D)[2–8].

Meanwhile, quasiperiodic systems have been intensively studied as they lie between periodic crystalline and disordered systems [9–11]. Presence of long-range order but lack of translational symmetry result in intriguing localization properties in quasiperiodic systems. Unlike purely random systems, quasiperiodic models can exhibit a distinct metal-insulator transition, separating extended and localized phases. Aubry and André studied a tight-binding model with incommensurately periodic on-site potential in 1D, showing that states could be either extended or localized, depending on the strength of on-site potential [12]. This model, now known as Aubry-André (AA) model, has a duality between the real space representation and momentum representation that rules out the existence of a mobility edge (ME) nevertheless. By introducing exponential hopping [13] or power-law hopping [14], or other ways to break the self-duality of

AA model [15–21], one is able to find MEs even in one-dimensional systems. Extending these concepts to 2D and continuous systems introduces new complexity. Quasicrystals show discrete rotation symmetries that are incompatible with translational symmetry [22]. Experiments and numerical simulations in quasicrystals have revealed the existence of MEs, typically characterized by localized states at lower energies and extended states at higher energies [23–27].

A third type of states known as critical states, which are extended but non-ergodic, are also studied in diverse quasiperiodic systems [27–35]. These states extend over a finite fraction of the system but remain non-uniform and fractal, displaying scaling behavior distinct from both localized and fully ergodic extended states. Existence of critical states has been verified across various platforms, including [36–51], photonic crystals [52], optical cavities [53, 54] and superconducting qubits [55, 56].

It has also been found that correlated random potentials can hold MEs even in one dimension, where all states would otherwise localize for uncorrelated disorder [57–59]. These results highlight that not only the disorder strength but also its correlation structure governs wave transport.

AL on hierarchical lattices such as the Bethe lattice (BL) has also been studied [60–66]. The motivation to study Anderson localization on the Cayley tree has been revived recently by the question of many-body local-

ization. Extended ergodic states, extended non-ergodic (critical) states and localized states were argued to exist for a range of disorder strength and energy [67].

In this letter, a unique 2D aperiodic potential that differs from both amorphous random disorder and rotationally symmetric quasicrystals is investigated. The potential is a random superposition of plane waves of a fixed wavevector magnitude  $q$  and has long range order. We call this a ‘‘Berry crystal,’’ a function introduced in connection with wave chaos [68, 69]. It is experimentally realizable in a laser cavity with a single mode laser with rough or ballistically chaotic walls, so that the wave inside is a random superposition of waves traveling in all directions. This potential has both short range and long range order and supports Bragg scattering of waves [70]. By analyzing the propagation of wavepackets within this type of potential, the energy spectrum is extracted from the autocorrelation function following a spectral method based on the simulation of wavepacket dynamics [71]. The finite size scaling analysis of eigenstates reveals changes from ergodic extended states to non-ergodic extended states and to Anderson localized states, rather than a simple sharp ME. At low potential strengths, an ergodic transition from low energy ergodic states to higher energy critical states near the backscattering momentum  $k = \frac{1}{2}q$  is observed. As the potential strength increases to become comparable to the backscattering energy, Anderson transition from low energy critical states to higher energy localized states is observed.

The Hamiltonian in momentum space is mapped onto an effective tight binding Cayley tree model. The mapping provides a natural interpretation for the non-ergodic extended states and give an estimation for the boundary of extended regimes below and above the backscattering energy.

## MODEL

We consider a single particle propagating in a 2D aperiodic potential. The Hamiltonian of the system in atomic units is given by

$$H = -\frac{\hbar^2}{2m}\nabla^2 + U(\mathbf{r}; \{\phi_j\}), \quad (1)$$

with the potential

$$U(\mathbf{r}; \{\phi_j\}) = \frac{\beta}{\sqrt{N/2}} \sum_{j=1}^N \cos(\mathbf{q}_j \cdot \mathbf{r} + \phi_j) \quad (2)$$

where  $m$  is the particle mass,  $\beta$  is the strength of potential,  $N$  is the number of modes,  $\mathbf{q}_j = q \cdot (\hat{x} \cos \theta_j + \hat{y} \sin \theta_j)$  are wave-vectors with fixed magnitude, and  $\theta_j$  are angles taken to be randomly distributed within  $[0, 2\pi]$ . The

root-mean-square of the potential is normalized as follows

$$U_{\text{rms}} = \sqrt{\langle U(\mathbf{r})^2 \rangle} = \beta. \quad (3)$$

This random potential has both short range order and long range order. The autocorrelation function  $C(\delta r)$  of the potential does not decay to zero in large distance limit for finite  $N$ , but in the limit of many modes  $N \rightarrow \infty$ ,  $C(\delta r)$  decay by power law with distance [70]. Dimensionless energy, length, and time are used based on the system’s inherent backscattering dynamics. We use recoil energy  $E_0 = \frac{\hbar^2 q^2}{8m}$  as energy units, wavelength  $a = \frac{2\pi}{q}$  as length units, and  $\frac{\hbar}{E_0}$  as time units.

The dynamics of the system with size  $L = 320$  are simulated by discretizing the spatial and temporal grids, and imposing a absorbing boundary condition. The system is allowed to evolve for a total dimensionless time  $T = 11,000$  with the third-order scheme, namely

$$e^{-iH\tau} = e^{-iU\tau/2} e^{-iK\tau} e^{-iU\tau/2} \quad (4)$$

where  $e^{-iH\tau}$  is the unitary evolution for each time step  $\tau$ , and  $K, U$  are the kinetic energy and potential energy respectively. The wave function at  $t = 0$  is taken to be a minimum uncertainty wavepacket, having the form:

$$\psi(\mathbf{r}) = A e^{-\left(\frac{(x-x_0)^2}{2\sigma_x^2} + \frac{(y-y_0)^2}{2\sigma_y^2}\right)} e^{i\mathbf{k}_0 \cdot \mathbf{r}} \quad (5)$$

The expectation value of  $\mathbf{r}$  and  $\mathbf{p}$  at  $t = 0$  equals to  $(0, 0)$  and  $\mathbf{k}_0$  respectively, while the width of wavepacket is fixed at  $\sigma_x = \sigma_y = 2$ .

The spectrum of the full system is inferred from taking the sum of Gaussian wavepackets with different initial position and momentum. We compute the autocorrelation of the wavepacket at over time and Fourier transform to obtain the power spectrum of the wavepacket [71]. Assuming time reversal symmetry, we have

$$|\langle \epsilon_n | \psi \rangle|^2 \propto \lim_{T \rightarrow \infty} \frac{1}{T} \text{Re} \left[ \int_0^T \langle \psi(0) | \psi(t) \rangle e^{i\epsilon_n t} dt \right] \quad (6)$$

In Fig. 1a, we plot the weighted density of states ( $\rho(\epsilon)$ ) defined as product of total simulation time and the Fourier transform of autocorrelation

$$\rho(\epsilon) = \text{Re} \left[ \int_0^{T'} \langle \psi(0) | \psi(t) \rangle e^{i\epsilon t} dt \right] \quad (7)$$

with system parameters  $(N, \beta) = (100, 0.6)$  and initial momentum  $k = 1/2 q$ . Different colors correspond to different integration time window  $T'$ : blue, red lines corresponds to  $T' = T/3, T$  respectively. The eigenstates are calculated by projections of wavepacket onto a very narrow energy range of order  $\frac{1}{T}$  using wavepacket dynamics

$$|\psi_\epsilon\rangle \propto \int_0^T e^{i\epsilon t} |\psi(t)\rangle dt \quad (8)$$

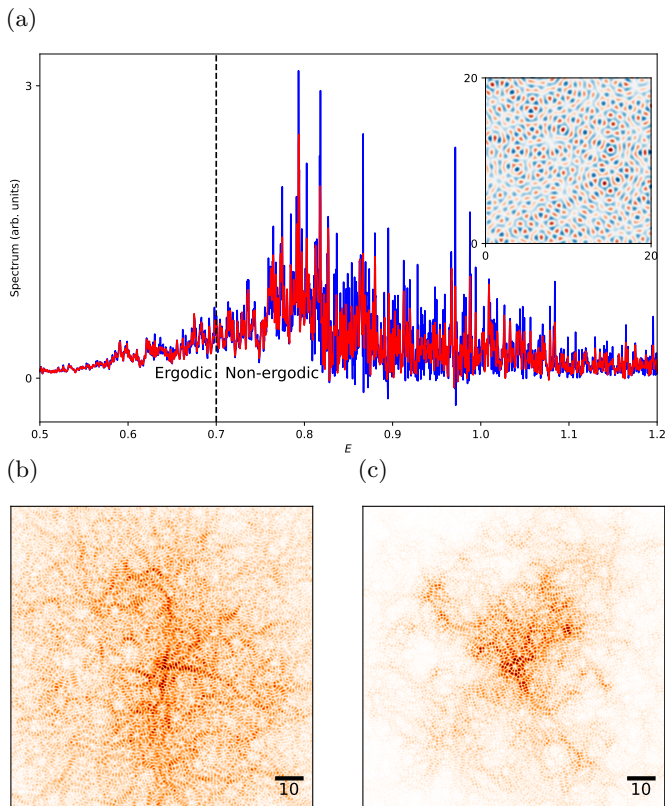


FIG. 1: (a) Spectrum obtained from  $\beta = 0.60, N = 100$  using a Gaussian wavepacket as initial state. The simulation time is taken to be  $T' = 11000$ . The red solid line represents the energy spectrum with integration time window  $T'/3$ , while the blue solid line corresponds to full time window  $T'$ . Ergodic states live in the part of spectrum that is invariant as the size of time window increases. The dashed line at  $E_c = 0.7$  is a guide for eye for the transition from the ergodic regime to the non-ergodic regime. The inset shows part of the 2D random potential  $V(x, y)$  generated by the superposition of the  $N = 100$  plane waves, in a  $20a \times 20a$  window. Energy eigenstates obtained from wavepacket dynamics at energies of  $\epsilon = 0.66, 1.00$  are plotted in (b) and (c), and the bars have lengths of  $10a$ . They correspond to extended and critical states respectively. Critical state has regions with high probability density, but they do not spread over the whole window. Extended state has regions with high probability density spread uniformly. The resolved eigenstates from Gaussian wavepacket have probability concentrated near origin and fade near boundaries because of memory of initial state and absorbing boundary condition.

The eigenstates obtained at energies  $\epsilon = 0.66, 1.00$  are plotted in Fig. 1b and Fig. 1c and correspond to extended and critical regions respectively. The critical state shows regions with high probability density, but they do not spread over the whole system.

These results indicate a transition from extended states to critical states at  $E \approx 0.7$ . In the low energy interval the  $\rho(\epsilon)$  in Eqn. 7 is invariant as the time window increases, corresponding to the behavior of an absolute

continuous spectrum. However, in the high energy interval,  $\rho(\epsilon)$  peaks grow taller and narrower as the time window increases, yet the growth of height is sublinear. This suggests that they belong to a singular continuous spectrum [54, 72]. The eigenstate is not localized but shows concentrated probability density only in some regions. To better analyze the transition and its dependence on  $\beta$  and  $N$ , we solved eigenstates using the Lanczos iterative eigensolver [73] with Dirichlet boundary condition.

Simulations on finite systems inevitably introduce edge states, which are states localized at the boundaries and therefore vanish in the thermodynamic limit. To systematically exclude them, we adopt the "binary map" filtering technique by Zhu et al. [27]. After excluding the edge states, we analyze the scaling of the Inverse Participation Ratio (IPR) with system size  $L$ . The IPR for a normalized state is defined as:

$$\text{IPR} = \int |\psi(\mathbf{r})|^4 d\mathbf{r} \quad (9)$$

For finite systems, the IPR scales as  $P^{-1} \propto L^{-\gamma}$ . The scaling exponent  $\gamma$  serves as a distinct order parameter. In the case of 2D systems,  $\gamma \approx 2$  indicates extended states,  $\gamma \approx 0$  indicates localized states as the support is independent of  $L$ , and intermediate values  $0 < \gamma < 2$  signify critical states with multifractal properties. We perform the Lanczos diagonalization for a range of system sizes  $L \in [200, 600]$  and calculate the averaged IPR,  $\overline{P^{-1}}$  within narrow energy windows  $\delta\epsilon = 1.5 \times 10^{-3}$  near a target energy  $E$ . The exponent  $\gamma$  is then obtained through a linear fit of  $\ln(\overline{P^{-1}})$  versus  $\ln L$ . The top row of Fig. 2 shows the scaling relations at different target energies for  $\beta = 0.4$ . As energy increases, transitions from extended state to critical state and back to extended state are clearly noted. The bottom row of Fig. 2 shows the scaling relations for  $\beta = 0.8$ , with low energy state being extended, state near backscattering energy being localized, and state of higher energy being critical. Examples of eigenstates are shown in Fig. 3.

By repeating this procedure across a grid of energy targets  $E$  and system parameters  $(\beta, N)$ , we find that  $\gamma$  is largely independent of  $N \in [20, 400]$ . Thus, we plot the  $\gamma(E, \beta)$  in Fig. 4. This map clearly shows different regions and the transitions. For weak potential ( $\beta \leq 0.7$ ), a transition from low energy extended states to critical states occurs near  $E = E_0$ . The extended region shrink and the critical region grow with potential strength until  $\beta \approx 0.7$ , where the localized states first appear. For  $\beta \geq 0.8$ , low energy extended states and high energy localized regions are separated by an intermediate critical region.

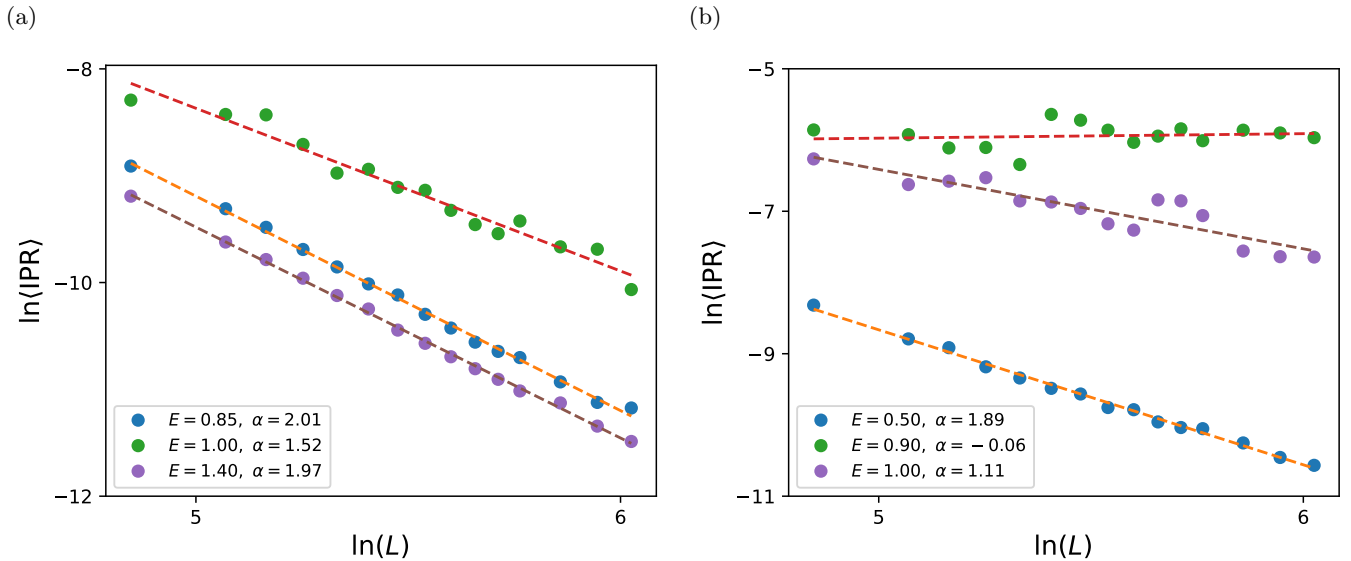


FIG. 2: Localization properties of states with different energies for different potential strength  $\beta$  can be inferred from scaling of IPRs.  $\ln(\overline{P^{-1}})$  are plotted against  $\ln L$  with  $L$  ranging from 200 to 600. Top row shows scaling relation for  $\beta = 0.4$  and  $N = 100$ . (a) Extended, target energy  $E = 0.85$  scaling exponent  $\gamma = 2.01 \pm 0.03$ . (b) Critical, target energy  $E = 1.0$  scaling exponent  $\gamma = 1.52 \pm 0.08$ . (c) Extended, target energy  $E = 1.4$  scaling exponent  $\gamma = 1.97 \pm 0.02$ . Bottom row shows scaling relation for  $\beta = 0.8$  and  $N = 100$ . (d) Extended, target energy  $E = 0.5$  scaling exponent  $\gamma = 1.89 \pm 0.04$ . (e) Localized, target energy  $E = 0.9$  scaling exponent  $\gamma = -0.06 \pm 0.14$ . (f) Critical, target energy  $E = 1.0$  scaling exponent  $\gamma = 1.11 \pm 0.15$ .

### BETHE LATTICE

The Hamiltonian written in momentum basis  $|\mathbf{k}\rangle$  is

$$\begin{aligned} \langle \mathbf{k} | H | \mathbf{k}' \rangle &= \delta_{\mathbf{k}, \mathbf{k}'} \frac{\hbar^2 k^2}{2m} + \frac{\beta}{2} \sum_j [e^{i\phi_j} \delta_{\mathbf{k}', \mathbf{k} + \mathbf{q}_j} + e^{-i\phi_j} \delta_{\mathbf{k}', \mathbf{k} - \mathbf{q}_j}] \\ &= \delta_{\mathbf{k}, \mathbf{k}'} \epsilon_{\mathbf{k}} + V_{\mathbf{k}, \mathbf{k}'}. \end{aligned} \quad (10)$$

Therefore, the potential induces hopping in momentum space by vectors  $\pm \mathbf{q}_j$ . The problem becomes a tight-binding model on a highly connected graph in momentum space. The structure of eigenstate at a given energy  $E$  is determined by the equation

$$(E - \epsilon_{\mathbf{k}}) c_{\mathbf{k}} = \sum_{\mathbf{k}'} V_{\mathbf{k}\mathbf{k}'} c'_{\mathbf{k}'}. \quad (11)$$

Components with momenta  $\mathbf{k}$  with  $|\epsilon_{\mathbf{k}} - E| \lesssim |V|$  carry the most of the weight. The eigenenergy thus defines a momentum shell, and components outside the shell are suppressed by large energy detunings. With a fixed energy  $E = E_{k_0}$ , the Hamiltonian can be projected onto a thin annulus in 2D momentum space. The projected Hamiltonian acts on momentum states lying close to the circle  $|\mathbf{k}| = k_0$ . The diagonal terms correspond on-site energies  $\epsilon_{\mathbf{k}}$ , while off-diagonal terms with constant amplitude correspond to hopping between sites whose momentum difference equals one of the  $\mathbf{q}_j$ .

The key quantity controlling the structure of the effective graph is the energy mismatch associated with a scattering  $\mathbf{k} \rightarrow \mathbf{k} + \mathbf{q}$ :

$$\Delta E(\mathbf{k}, \mathbf{q}) = \frac{|\mathbf{k} + \mathbf{q}|^2 - k_0^2}{2m} = \frac{q^2}{2m} + \frac{k_0 q}{m} \cos \theta, \quad (12)$$

where  $\theta$  is the angle between  $\mathbf{k}$  and  $\mathbf{q}$ . For  $k_0 > q/2$ , the equation  $\cos \theta_0 = \frac{q}{2k_0}$  has two real solutions which give two Bragg angles. Since the potential has only a finite number of peaks in momentum space, the scattering is never perfectly resonant. For each Bragg angle, there are two nearly resonant scattering processes. Therefore, each momentum  $\mathbf{k}$  is connected to four neighbors by nearly resonant scattering processes. Repeated scattering generates a Cayley tree structure because loops are prevented by the incommensurate random  $\mathbf{q}_j$  and each momentum have the same local connectivity. The effective graph is a Cayley tree with branching number  $K \simeq 3$ .

The onsite energy of a state on this BL is given by the Bragg angle and angle detuning  $\delta\theta$

$$\epsilon_{\mathbf{k}} \sim E_{k_0} + 2k_0 q \sin \theta_0 \delta\theta \sim E_{k_0} + 8E_0 \sqrt{E_{k_0}/E_0 - 1} \delta\theta, \quad (13)$$

for small  $\delta\theta$ , where  $E_0$  is the recoil energy. After subtracting the constant shift  $E_{k_0}$  from onsite energy, the effective Hamiltonian is reduced to Anderson model on a

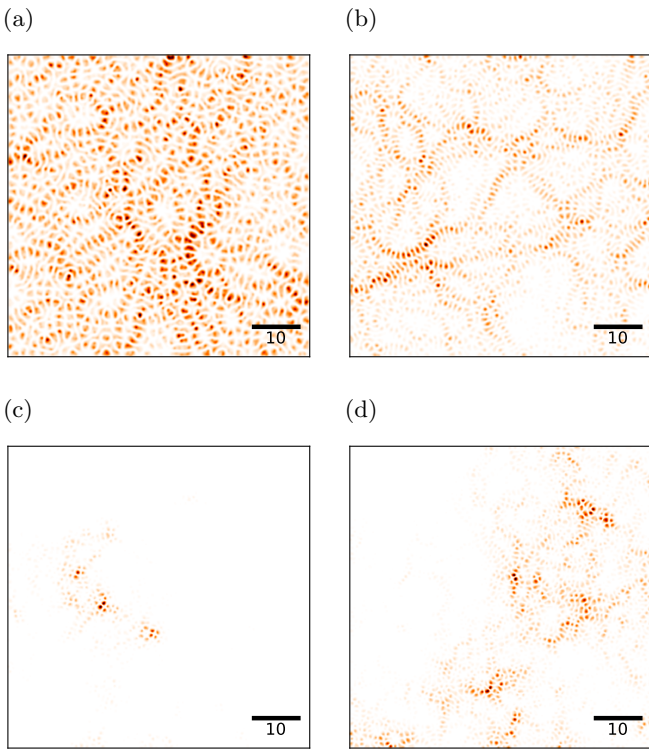


FIG. 3: Eigenstates in various energy ranges and potential strength are plotted, and the bars have lengths of  $10a$ . Top row shows the probability density of energy eigenstates for  $\beta = 0.4$  and  $N = 100$ . (a) States are extended at  $\epsilon = 0.5$ . (b) States are critical at  $\epsilon = 0.85$ . There are regions with high probability density, but they do not spread over the whole space. Top row shows that  $\beta = 0.8$  and  $N = 100$ . (c) States are localized at  $\epsilon = 0.9$ . Probability density is concentrated in small regions, which do not percolate. (d) States are critical at  $\epsilon = 1.2$ .

Carley tree

$$H_{\text{eff}}^{(k > q/2)} = \sum_i^N \epsilon_i |i\rangle\langle i| + \sum_{\langle i,j \rangle} t e^{i\phi_{ij}} |i\rangle\langle j| + \text{h.c.}, \quad (14)$$

where  $t = \beta/\sqrt{2N}$  is the constant hopping amplitude,  $\phi_{ij}$  are random phases,  $\epsilon_i$  are random onsite energies, and the sum is over nearest neighbor sites. Higher order terms in the perturbation theory can be ignored in the weak potential limit.

For  $k_0 < q/2$ , the resonance condition in equation 12 has no solution. All first order scatterings are off-shell, with the smallest energy detuning  $\Delta_1 = 4(1 - \sqrt{E})$  in unit of the recoil energy  $E_0$ , where  $E$  is the eigenenergy in unit of  $E_0$ . The leading resonant processes occur at second order with hopping amplitude  $t_{\text{eff}} \sim \frac{\beta^2}{8N(1-\sqrt{E})}$  and onsite energy  $\epsilon = 4(2 - \sqrt{E})(\delta\theta)^2 \propto \frac{1}{N^2}$ . For large enough  $N$ , second order processes always dominate over first order scatterings. The second order process also

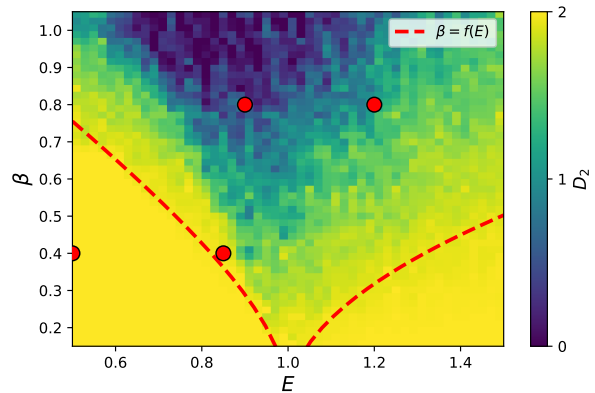


FIG. 4: Phase diagram of the localization transition in the energy-disorder plane  $(E, \beta)$ . The color map displays the fractal dimension  $D_2$ , extracted from the finite-size scaling of the IPR,  $P^{-1} \sim L^{-D_2}$ . The extended phase is characterized by  $D_2 \approx 2$  (yellow regions), while  $D_2 < 2$  (blue to green gradients) indicates the onset of critical or localized behavior. For weak potential ( $\beta \leq 0.6$ ), a transition from low energy extended states to critical states occurs near  $E = 0.9$ . For  $\beta \geq 0.8$ , a transition from low energy extended states to critical states occurs near  $E = 0.7$ . The superimposed red dashed line marks the theoretical estimate of the ergodic transition based on the mapping onto a Cayley tree in momentum space. The V-shaped dip centered at  $E \approx 1$  highlights the back-scattering resonance, where the system is most susceptible to localization. The red circles are eigenstates presented in figure 2.

connects each momentum state to four neighbors, so the effective Hamiltonian has the same format as in equation 14 but with different  $t$  and  $\epsilon_i$ .

BL support extended, critical (non-ergodic), and localized phases. The phase is characterised by the fractal dimensions of the eigenstates, which depend on disorder. For a BL model with  $t = 1$  and  $\epsilon_i$  uniformly distributed in the interval  $(-W/2, W/2)$ , non-ergodic extended phase exist in range  $W_E < W < W_C$  [64, 67]. Anderson localization transition happens at  $W = W_C$  and ergodic transition at  $W = W_E$ . States are localized for  $W > W_C$  and are ergodic for  $W < W_E$ .  $W_E$  and  $W_C$  depends on the connectivity  $K$ . For a BL with Cauchy disorder

$$P_{\text{Cauchy}}(\epsilon) = \frac{W}{\pi(\epsilon^2 + W^2)}, \quad (15)$$

a critical disorder width  $W_C$  at the center of the band  $E = 0$  has also been found. The spread of the disorder and  $K$  determine the fractal dimension of states. In this Cayley tree mapping, the distribution of onsite energy  $\epsilon$  is estimated using 5,000 realizations of the potential in equation 2. For  $k_0 > q/2$ ,  $\epsilon$  is observed to follow a Gaussian distribution with the standard deviation  $\sim 8\sqrt{E-1} \frac{0.4\pi}{N}$ . For  $k_0 < q/2$ ,  $\epsilon$  follows an exponential decay with the standard deviation  $\sim 4(2 - \sqrt{E}) (\frac{1.7\pi}{N})^2$ .

The effective Hamiltonian in equation 14 can be normalized to have unity hopping amplitude. The standard

deviation of disorder  $W$  is then a function of  $E$  and  $\beta$ . Thus, by solving  $W(E, \beta) = W_C$ , the boundary between extended and critical states in  $E - \beta$  plane can be obtained.

$$W_C = \frac{46\pi^2(2 - \sqrt{E})(1 - \sqrt{E})}{N\beta^2}, E > E_0$$

$$W_C = \frac{3.2\pi}{\beta} \sqrt{2(E - 1)/N}, E < E_0$$
(16)

A localized (extended) state in momentum space exhibits an extended (localized) distribution in real space. Multifractal states, however, exhibit delocalized yet non-ergodic behavior in both real and momentum spaces. Fractal dimension for the BL model can therefore map out the nature of states in real space. States far away from backscattering energy have large  $W$  and are therefore localized in momentum space and extended in real space. States closer to backscattering energy have smaller  $W$  and are non-ergodic extended states in both momentum and real space.  $W_C \sim 6$  gives the observed boundary between ergodic extended states and non-ergodic extended states in real space, as shown in figure 4. This agrees with values in literatures for  $K = 3$  [60, 65]. It has to be noted that the mapping is not valid in the limit of  $N \rightarrow \infty$  because it only considers first order and second order scatterings. As  $N \rightarrow \infty$ , higher order virtual process must also be considered as energy detunings become vanishingly small. The scaling of  $\beta \propto \frac{1}{\sqrt{N}}$  (eq 16) is only valid up to  $N \sim 100$  from the finite size scaling analysis of IPR.

## CONCLUSION AND DISCUSSION

We have proposed a novel 2D model with superpositions of fixed-wavevector sinusoidal potential as disorder. This system, with long range order but lack of translational and rotational symmetry, holds extended, critical, and localized states. When the typical potential fluctuation is much smaller than the recoil energy, a transition from low-energy extended states and critical states around recoil energy. As the typical size of potential increases, the low-energy states are critical, and the states near backscattering momentum are Anderson localized. We developed numerical methods to simulate and analyze the 2D quantum dynamics, as well as theoretical tools to estimate the energy and disorder strength of ergodic transition. A further intriguing issue is to analyze the transport properties in interacting systems with additional particle-particle interactions and particle-background couplings. The back-scattering momentum coincides with the concept of nesting vectors on Fermi surfaces, and we expect that this letter could provide further insights on the charge density wave phase and pseudogap phase of strange metals.

## ACKNOWLEDGEMENTS

The authors thank Xinchu Zhou, Zhongling Lu, Mingxuan Xiao, Yubo Zhang, Jasper Jain for discussion and suggestion. We thank the NSF Center for Integrated Quantum Materials (CIQM) Grant No. DMR-1231319.

---

\* zc362@cam.ac.uk

† alaincsy@stu.pku.edu.cn

‡ chenzhengyu@stu.pku.edu.cn

§ eheller@fas.harvard.edu

- [1] P. W. Anderson, Absence of Diffusion in Certain Random Lattices, *Physical Review* **109**, 1492 (1958).
- [2] F. Evers and A. D. Mirlin, Anderson transitions, *Reviews of Modern Physics* **80**, 1355 (2008).
- [3] J. Chabé, G. Lemarié, B. Grémaud, D. Delande, P. Szriftgiser, and J. C. Garreau, Experimental Observation of the Anderson Metal-Insulator Transition with Atomic Matter Waves, *Physical Review Letters* **101**, 255702 (2008).
- [4] D. J. Thouless, Electrons in disordered systems and the theory of localization, *Physics Reports* **13**, 93 (1974).
- [5] P. W. Anderson, D. J. Thouless, E. Abrahams, and D. S. Fisher, New method for a scaling theory of localization, *Physical Review B* **22**, 3519 (1980).
- [6] D. H. White, T. A. Haase, D. J. Brown, M. D. Hoogerland, M. S. Najafabadi, J. L. Helm, C. Gies, D. Schumayer, and D. A. W. Hutchinson, Observation of two-dimensional Anderson localisation of ultracold atoms, *Nature Communications* **11**, 4942 (2020).
- [7] E. Abrahams, P. W. Anderson, D. C. Licciardello, and T. V. Ramakrishnan, Scaling Theory of Localization: Absence of Quantum Diffusion in Two Dimensions, *Physical Review Letters* **42**, 673 (1979).
- [8] T. Schwartz, G. Bartal, S. Fishman, and M. Segev, Transport and Anderson localization in disordered two-dimensional photonic lattices, *Nature* **446**, 52 (2007).
- [9] D. Shechtman, I. Blech, D. Gratias, and J. W. Cahn, Metallic phase with long-range orientational order and no translational symmetry, *Phys. Rev. Lett.* **53**, 1951 (1984).
- [10] G. Roux, T. Barthel, I. P. McCulloch, C. Kollath, U. Schollwöck, and T. Giamarchi, Quasiperiodic bose-hubbard model and localization in one-dimensional cold atomic gases, *Phys. Rev. A* **78**, 023628 (2008).
- [11] Crystallography of quasicrystals: Concepts, methods and structures, *Journal of the American Chemical Society* **132**, 5534 (2010), PMID: 20337474, <https://doi.org/10.1021/ja102189x>.
- [12] S. Aubry and G. André, Analyticity breaking and anderson localization in incommensurate lattices, *Proceedings, VIII International Colloquium on Group-Theoretical Methods in Physics* **3** (1980).
- [13] J. Biddle and S. Das Sarma, Predicted Mobility Edges in One-Dimensional Incommensurate Optical Lattices: An Exactly Solvable Model of Anderson Localization, *Physical Review Letters* **104**, 070601 (2010).
- [14] X. Deng, S. Ray, S. Sinha, G. V. Shlyapnikov, and L. Santos, One-Dimensional Quasicrystals with Power-Law Hopping, *Physical Review Letters* **123**, 025301

- (2019).
- [15] S. Ganesan, J. H. Pixley, and S. Das Sarma, Nearest Neighbor Tight Binding Models with an Exact Mobility Edge in One Dimension, *Physical Review Letters* **114**, 146601 (2015).
- [16] Y. Wang, X. Xia, L. Zhang, H. Yao, S. Chen, J. You, Q. Zhou, and X.-J. Liu, One-Dimensional Quasiperiodic Mosaic Lattice with Exact Mobility Edges, *Physical Review Letters* **125**, 196604 (2020).
- [17] S. Das Sarma, S. He, and X. C. Xie, Mobility Edge in a Model One-Dimensional Potential, *Physical Review Letters* **61**, 2144 (1988).
- [18] J. Biddle, B. Wang, D. J. Priour, and S. Das Sarma, Localization in one-dimensional incommensurate lattices beyond the Aubry-Andr\`e model, *Physical Review A* **80**, 021603 (2009).
- [19] X. Li, X. Li, and S. Das Sarma, Mobility edges in one-dimensional bichromatic incommensurate potentials, *Physical Review B* **96**, 085119 (2017).
- [20] M. Gonçalves, B. Amorim, E. Castro, and P. Ribeiro, Hidden dualities in 1D quasiperiodic lattice models, *SciPost Physics* **13**, 046 (2022).
- [21] S. Roy, T. Mishra, B. Tanatar, and S. Basu, Reentrant Localization Transition in a Quasiperiodic Chain, *Physical Review Letters* **126**, 106803 (2021).
- [22] M. Senechal and P. Paufler, Crystalline symmetries. an informal mathematical introduction. adam hilger, bristol, philadelphia, new york 1990. 137 p., £ 19.50. isbn 0-7503-0041-8, *Crystal Research and Technology* **28**, 304 (1993), <https://onlinelibrary.wiley.com/doi/pdf/10.1002/crat.2170280304>
- [23] P. Wang, Q. Fu, V. V. Konotop, Y. V. Kartashov, and F. Ye, Observation of localization of light in linear photonic quasicrystals with diverse rotational symmetries, *Nature Photonics* **18**, 224 (2024).
- [24] M. Sbroscia, K. Viebahn, E. Carter, J.-C. Yu, A. Gaunt, and U. Schneider, Observing Localization in a 2D Quasicrystalline Optical Lattice, *Physical Review Letters* **125**, 200604 (2020).
- [25] Y. S. Chan, C. T. Chan, and Z. Y. Liu, Photonic Band Gaps in Two Dimensional Photonic Quasicrystals, *Physical Review Letters* **80**, 956 (1998).
- [26] D. Levine and P. J. Steinhardt, Quasicrystals: A New Class of Ordered Structures, *Physical Review Letters* **53**, 2477 (1984).
- [27] Z. Zhu, S. Yu, D. Johnstone, and L. Sanchez-Palencia, Localization and spectral structure in two-dimensional quasicrystal potentials, *Phys. Rev. A* **109**, 013314 (2024).
- [28] T. Liu, X. Xia, S. Longhi, and L. Sanchez-Palencia, Anomalous mobility edges in one-dimensional quasiperiodic models, *SciPost Physics* **12**, 027 (2022).
- [29] H. Yao, A. Khoudli, L. Bresque, and L. Sanchez-Palencia, Critical Behavior and Fractality in Shallow One-Dimensional Quasiperiodic Potentials, *Physical Review Letters* **123**, 070405 (2019).
- [30] V. Goblot, A. Štrkalj, N. Pernet, J. L. Lado, C. Dorow, A. Lemaître, L. Le Gratiet, A. Harouri, I. Sagnes, S. Ravets, A. Amo, J. Bloch, and O. Zilberberg, Emergence of criticality through a cascade of delocalization transitions in quasiperiodic chains, *Nature Physics* **16**, 832 (2020).
- [31] N. Roy and A. Sharma, Fraction of delocalized eigenstates in the long-range Aubry-Andr\`e-Harper model, *Physical Review B* **103**, 075124 (2021).
- [32] M. Gonçalves, B. Amorim, E. V. Castro, and P. Ribeiro, Critical Phase Dualities in 1D Exactly Solvable Quasiperiodic Models, *Physical Review Letters* **131**, 186303 (2023).
- [33] J. Fraxanet, U. Bhattacharya, T. Grass, M. Lewenstein, and A. Dauphin, Localization and multifractal properties of the long-range Kitaev chain in the presence of an Aubry-Andr\`e-Harper modulation, *Physical Review B* **106**, 024204 (2022).
- [34] Y. Wang, L. Zhang, W. Sun, T.-F. J. Poon, and X.-J. Liu, Quantum phase with coexisting localized, extended, and critical zones, *Physical Review B* **106**, L140203 (2022).
- [35] C. W. Duncan, Critical states and anomalous mobility edges in two-dimensional diagonal quasicrystals, *Phys. Rev. B* **109**, 014210 (2024).
- [36] G. Roati, C. D'Errico, L. Fallani, M. Fattori, C. Fort, M. Zaccanti, G. Modugno, M. Modugno, and M. Inguscio, Anderson localization of a non-interacting Bose-Einstein condensate, *Nature* **453**, 895 (2008).
- [37] P. Bordia, H. P. Lüschen, S. S. Hodgman, M. Schreiber, I. Bloch, and U. Schneider, Coupling Identical one-dimensional Many-Body Localized Systems, *Physical Review Letters* **116**, 140401 (2016).
- [38] F. A. An, E. J. Meier, and B. Gadway, Engineering a Flux-Dependent Mobility Edge in Disordered Zigzag Chains, *Physical Review X* **8**, 031045 (2018).
- [39] R. C. Kuhn, C. Miniatura, D. Delande, O. Sigwarth, and C. A. Müller, Localization of Matter Waves in Two-Dimensional Disordered Optical Potentials, *Physical Review Letters* **95**, 250403 (2005).
- [40] S. Lellouch and L. Sanchez-Palencia, Localization transition in weakly interacting Bose superfluids in one-dimensional quasiperiodic lattices, *Physical Review A* **90**, 061602 (2014).
- [41] D. J. Boers, B. Goedeke, D. Hinrichs, and M. Holthaus, Mobility edges in bichromatic optical lattices, *Physical Review A* **75**, 063404 (2007).
- [42] C. D'Errico, E. Lucioni, L. Tanzi, L. Gori, G. Roux, I. P. McCulloch, T. Giamarchi, M. Inguscio, and G. Modugno, Observation of a Disordered Bosonic Insulator from Weak to Strong Interactions, *Physical Review Letters* **113**, 095301 (2014).
- [43] M. Cutler and N. F. Mott, Observation of Anderson Localization in an Electron Gas, *Physical Review* **181**, 1336 (1969).
- [44] Y. Wang, J.-H. Zhang, Y. Li, J. Wu, W. Liu, F. Mei, Y. Hu, L. Xiao, J. Ma, C. Chin, and S. Jia, Observation of Interaction-Induced Mobility Edge in an Atomic Aubry-Andr\`e Wire, *Physical Review Letters* **129**, 103401 (2022).
- [45] M. Schreiber, S. S. Hodgman, P. Bordia, H. P. Lüschen, M. H. Fischer, R. Vosk, E. Altman, U. Schneider, and I. Bloch, Observation of many-body localization of interacting fermions in a quasirandom optical lattice, *Science* **349**, 842 (2015).
- [46] H. P. Lüschen, P. Bordia, S. Scherg, F. Alet, E. Altman, U. Schneider, and I. Bloch, Observation of Slow Dynamics near the Many-Body Localization Transition in One-Dimensional Quasiperiodic Systems, *Physical Review Letters* **119**, 260401 (2017).
- [47] P. Bordia, H. Lüschen, S. Scherg, S. Gopalakrishnan, M. Knap, U. Schneider, and I. Bloch, Probing Slow Relaxation and Many-Body Localization in Two-Dimensional Quasiperiodic Systems, *Physical Review X*

- 7, 041047 (2017).
- [48] Y. Wang, L. Zhang, S. Niu, D. Yu, and X.-J. Liu, Realization and Detection of Nonergodic Critical Phases in an Optical Raman Lattice, *Physical Review Letters* **125**, 073204 (2020).
- [49] H. P. Lüschen, S. Scherg, T. Kohlert, M. Schreiber, P. Bordia, X. Li, S. Das Sarma, and I. Bloch, Single-Particle Mobility Edge in a One-Dimensional Quasiperiodic Optical Lattice, *Physical Review Letters* **120**, 160404 (2018).
- [50] L. Fallani, J. E. Lye, V. Guarrera, C. Fort, and M. Inguscio, Ultracold Atoms in a Disordered Crystal of Light: Towards a Bose Glass, *Physical Review Letters* **98**, 130404 (2007).
- [51] F. A. An, K. Padavić, E. J. Meier, S. Hegde, S. Ganesan, J. H. Pixley, S. Vishveshwara, and B. Gadway, Interactions and Mobility Edges: Observing the Generalized Aubry-André Model, *Physical Review Letters* **126**, 040603 (2021).
- [52] Y. Lahini, R. Pugatch, F. Pozzi, M. Sorel, R. Morandotti, N. Davidson, and Y. Silberberg, Observation of a Localization Transition in Quasiperiodic Photonic Lattices, *Physical Review Letters* **103**, 013901 (2009).
- [53] R. Dalichaouch, J. P. Armstrong, S. Schultz, P. M. Platzman, and S. L. McCall, Microwave localization by two-dimensional random scattering, *Nature* **354**, 53 (1991).
- [54] D. Tanese, E. Gurevich, F. Baboux, T. Jacqmin, A. Lemaître, E. Galopin, I. Sagnes, A. Amo, J. Bloch, and E. Akkermans, Fractal Energy Spectrum of a Polariton Gas in a Fibonacci Quasiperiodic Potential, *Physical Review Letters* **112**, 146404 (2014).
- [55] H. Li, Y.-Y. Wang, Y.-H. Shi, K. Huang, X. Song, G.-H. Liang, Z.-Y. Mei, B. Zhou, H. Zhang, J.-C. Zhang, S. Chen, S. P. Zhao, Y. Tian, Z.-Y. Yang, Z. Xiang, K. Xu, D. Zheng, and H. Fan, Observation of critical phase transition in a generalized Aubry-André-Harper model with superconducting circuits, *npj Quantum Information* **9**, 1 (2023).
- [56] P. Roushan, C. Neill, J. Tangpanitanon, V. M. Bastidas, A. Megrant, R. Barends, Y. Chen, Z. Chen, B. Chiaro, A. Dunsworth, A. Fowler, B. Foxen, M. Giustina, E. Jeffrey, J. Kelly, E. Lucero, J. Mutus, M. Neeley, C. Quintana, D. Sank, A. Vainsencher, J. Wenner, T. White, H. Neven, D. G. Angelakis, and J. Martinis, Spectroscopic signatures of localization with interacting photons in superconducting qubits, *Science* **358**, 1175 (2017).
- [57] L. Tessieri, Delocalization phenomena in one-dimensional models with long-range correlated disorder: a perturbative approach, *Journal of Physics A: Mathematical and General* **35**, 9585 (2002).
- [58] F. A. B. F. de Moura and M. L. Lyra, Delocalization in the 1d anderson model with long-range correlated disorder, *Phys. Rev. Lett.* **81**, 3735 (1998).
- [59] F. M. Izrailev and A. A. Krokhin, Localization and the mobility edge in one-dimensional potentials with correlated disorder, *Phys. Rev. Lett.* **82**, 4062 (1999).
- [60] R. Abou-Chacra, D. J. Thouless, and P. W. Anderson, A selfconsistent theory of localization, *Journal of Physics C: Solid State Physics* **6**, 1734 (1973).
- [61] K. S. Tikhonov and A. D. Mirlin, Fractality of wave functions on a cayley tree: Difference between tree and locally treelike graph without boundary, *Phys. Rev. B* **94**, 184203 (2016).
- [62] G. Parisi, S. Pascazio, F. Pietracaprina, V. Ros, and A. Scardicchio, Anderson transition on the bethe lattice: an approach with real energies, *Journal of Physics A: Mathematical and Theoretical* **53**, 014003 (2019).
- [63] A. De Luca, B. L. Altshuler, V. E. Kravtsov, and A. Scardicchio, Anderson localization on the bethe lattice: Nonergodicity of extended states, *Phys. Rev. Lett.* **113**, 046806 (2014).
- [64] B. L. Altshuler, E. Cuevas, L. B. Ioffe, and V. E. Kravtsov, Nonergodic phases in strongly disordered random regular graphs, *Phys. Rev. Lett.* **117**, 156601 (2016).
- [65] C. Monthus and T. Garel, Anderson localization on the cayley tree: multifractal statistics of the transmission at criticality and off criticality, *Journal of Physics A: Mathematical and Theoretical* **44**, 145001 (2011).
- [66] S. Savitz, C. Peng, and G. Refael, Anderson localization on the bethe lattice using cages and the wegner flow, *Phys. Rev. B* **100**, 094201 (2019).
- [67] V. Kravtsov, B. Altshuler, and L. Ioffe, Non-ergodic delocalized phase in anderson model on bethe lattice and regular graph, *Annals of Physics* **389**, 148 (2018).
- [68] M. V. Berry, Regular and irregular semiclassical wavefunctions, *Journal of Physics A: Mathematical and General* **10**, 2083 (1977).
- [69] M. S. Longuet-Higgins, The statistical analysis of a random, moving surface, *Philosophical Transactions of the Royal Society of London, Series A: Mathematical and Physical Sciences* **249**, 321 (1957), <https://royalsocietypublishing.org/rsta/article-pdf/249/966/321/266676/rsta.1957.0002.pdf>.
- [70] D. Kim and E. J. Heller, Bragg Scattering from a Random Potential, *Physical Review Letters* **128**, 200402 (2022).
- [71] M. D. Feit, J. A. Fleck, and A. Steiger, Solution of the Schrödinger equation by a spectral method, *Journal of Computational Physics* **47**, 412 (1982).
- [72] E. Akkermans, Fractal spectrum and quasi-periodic potential, Presentation at the 5th Cornell Conference on Analysis, Probability, and Mathematical Physics on Fractals (2014), available at <https://pi.math.cornell.edu/~fractals/5/Akkerman.pdf>.
- [73] C. Lanczos, An iteration method for the solution of the eigenvalue problem of linear differential and integral operators, *Journal of Research of the National Bureau of Standards* **45**, 255 (1950).